J|A|C|S ARTICLES

Published on Web 10/14/2010

Growth of Metal−Organic Frameworks on Polymer Surfaces

Andrea Centrone,[†,§] Ying Yang,[†,||] Scott Speakman,[‡] Lev Bromberg,[†] Gregory C. Rutledge,[†] and T. Alan Hatton*[,†]

Department of Chemical Engineering and Center for Materials Science and Engineering, Massachusetts Institute of Technology, 77 Massachusetts Avenue, Cambridge, Massachusetts 02139, United States

Received July 19, 2010; E-mail: tahatton@mit.edu

Abstract: Polymer substrates have been functionalized with a MOF material (MIL-47) synthesized directly on polyacrylonitrile using in situ microwave irradiation. The growth of MIL-47 on these substrates was studied as a function of microwave irradiation time using scanning electron microscopy, X-ray diffraction, Fourier transform infrared spectroscopy, and X-ray photoelectron spectroscopy. The conversion of nitrile to carboxylic acid groups on the PAN surface was necessary for the growth of MIL-47 on the substrate. MIL-47 crystals grew over time at the expense of a related disordered precursor phase, which lacks the long-range order of MIL-47. This work paves the way for the development of a new class of hybrid MOF-polymer materials that will extend the applications of MOFs to fields such as membrane separations, filtration, and protective textiles.

1. Introduction

Metal−organic frameworks (MOFs) are crystalline materials composed of organic linkers connecting small inorganic clusters, which form 3D porous networks.[1−3] The large surface area, accessible pore volume, chemical stability, and tailorable pore sizes and functionalities make MOF materials promising in applications such as hydrogen storage,[4−6] separation,[7] sequestration of harmful gases,[8] catalysis,[9] drug delivery,[10,11] and in vivo imaging.[11] Additionally, the incorporation of transition metal ions in the MOF structures gives these materials interesting optical,[12] electrochemical,[13] and magnetic properties.[14−16] Pioneering work reporting on the growth[17−24] or deposition[25] of MOF materials on solid surfaces has attracted great attention recently, because the preparation of MOF thin films promises to extend their applications to sensors,[21,23,24] membrane separations,[22] and catalytically active coatings.

In this work, a MOF material (MIL-47)[14,16] was synthesized directly on polyacrylonitrile (PAN) substrates using in situ microwave irradiation. MIL-47 consists of chains composed of corner-sharing vanadium(III) oxide octahedra connected by terephthalate linkers (Figure 1). The resulting framework is characterized by one-dimensional cavities that are filled by terephthalic acid molecules in the as-synthesized material.[14] We

[†] Department of Chemical Engineering.
[‡] Center for Materials Science and Engineering.
[§] Present address: Center for Nanoscale Science and Technology, National Institute of Standards and Technology, Gaithersburg, MD 20899.
[||] Present address: Department of Electrical Engineering, Tsinghua University, Beijing 100084, P. R. China.

(1) Eddaoudi, M.; Kim, J.; Rosi, N.; Vodak, D.; Wachter, J.; O'Keeffe, M.; Yaghi, O. M. *Science* **2002**, *295*, 469–472.
(2) Eddaoudi, M.; Moler, D. B.; Li, H. L.; Chen, B. L.; Reineke, T. M.; O'Keeffe, M.; Yaghi, O. M. *Acc. Chem. Res.* **2001**, *34*, 319–330.
(3) Ferey, G. *Chem. Soc. Rev.* **2008**, *37*, 191–214.
(4) Wong-Foy, A. G.; Matzger, A. J.; Yaghi, O. M. *J. Am. Chem. Soc.* **2006**, *128*, 3494–3495.
(5) Murray, L. J.; Dinca, M.; Long, J. R. *Chem. Soc. Rev.* **2009**, *38*, 1294–1314.
(6) Centrone, A.; Siberio-Perez, D. Y.; Millward, A. R.; Yaghi, O. M.; Matzger, A. J.; Zerbi, G. *Chem. Phys. Lett.* **2005**, *411*, 516–519.
(7) Alaerts, L.; Kirschhock, C. E. A.; Maes, M.; van der Veen, M. A.; Finsy, V.; Depla, A.; Martens, J. A.; Baron, G. V.; Jacobs, P. A.; Denayer, J. E. M.; De Vos, D. E. *Angew. Chem., Int. Ed.* **2007**, *46*, 4293–4297.
(8) Britt, D.; Tranchemontagne, D.; Yaghi, O. M. *Proc. Natl. Acad. Sci. U.S.A.* **2008**, *105*, 11623–11627.
(9) Lee, J.; Farha, O. K.; Roberts, J.; Scheidt, K. A.; Nguyen, S. T.; Hupp, J. T. *Chem. Soc. Rev.* **2009**, *38*, 1450–1459.
(10) Horcajada, P.; Serre, C.; Maurin, G.; Ramsahye, N. A.; Balas, F.; Vallet-Regi, M.; Sebban, M.; Taulelle, F.; Ferey, G. *J. Am. Chem. Soc.* **2008**, *130*, 6774–6780.
(11) Horcajada, P.; et al. *Nat. Mater.* **2010**, *9*, 172–178.
(12) Allendorf, M. D.; Bauer, C. A.; Bhakta, R. K.; Houk, R. J. T. *Chem. Soc. Rev.* **2009**, *38*, 1330–1352.
(13) Ferey, G.; Millange, F.; Morcrette, M.; Serre, C.; Doublet, M. L.; Greneche, J. M.; Tarascon, J. M. *Angew. Chem., Int. Ed.* **2007**, *46*, 3259–3263.
(14) Barthelet, K.; Marrot, J.; Riou, D.; Ferey, G. *Angew. Chem., Int. Ed.* **2002**, *41*, 281–284.
(15) Kurmoo, M. *Chem. Soc. Rev.* **2009**, *38*, 1353–1379.
(16) Centrone, A.; Harada, T.; Speakman, S.; Hatton, T. A. *Small* **2010**, *6*, 1598–1602.
(17) Shekhah, C.; Wang, H.; Kowarik, S.; Schreiber, F.; Paulus, M.; Tolan, M.; Sternemann, C.; Evers, F.; Zacher, D.; Fischer, R. A.; Woll, C. *J. Am. Chem. Soc.* **2007**, *129*, 15118–15119.
(18) Shekhah, O.; Wang, H.; Paradinas, M.; Ocal, C.; Schupbach, B.; Terfort, A.; Zacher, D.; Fischer, R. A.; Woll, C. *Nat. Mater.* **2009**, *8*, 481–484.
(19) Biemmi, E.; Scherb, C.; Bein, T. *J. Am. Chem. Soc.* **2007**, *129*, 8054–8055.
(20) Zacher, D.; Shekhah, O.; Woll, C.; Fischer, R. A. *Chem. Soc. Rev.* **2009**, *38*, 1418–1429.
(21) Allendorf, M. D.; Houk, R. J. T.; Andruszkiewicz, L.; Talin, A. A.; Pikarsky, J.; Choudhury, A.; Gall, K. A.; Hesketh, P. J. *J. Am. Chem. Soc.* **2008**, *130*, 14404–14405.
(22) Yoo, Y.; Jeong, H. K. *Chem. Commun.* **2008**, 2441–2443.
(23) Biemmi, E.; Darga, A.; Stock, N.; Bein, T. *Microporous Mesoporous Mater.* **2008**, *114*, 380–386.
(24) Zou, X. Q.; Zhu, G. S.; Hewitt, I. J.; Sun, F. X.; Qiu, S. L. *Dalton Trans.* **2009**, 3009–3013.
(25) Horcajada, P.; Serre, C.; Grosso, D.; Boissiere, C.; Perruchas, S.; Sanchez, C.; Ferey, G. *Adv. Mater.* **2009**, *21*, 1931–1935.

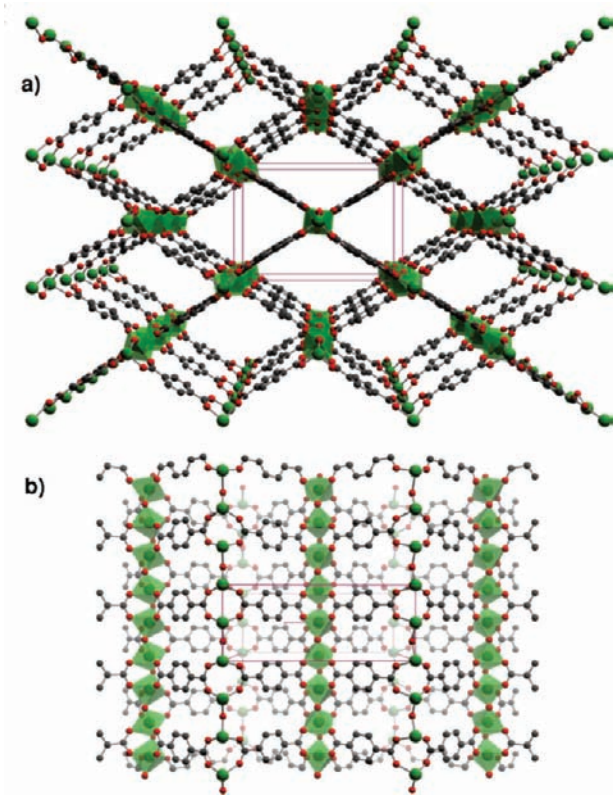

Figure 1. MIL-47 structure: view along the *b* axis (top) and along the *c* axis (bottom). Color code: green (vanadium), red (oxygen), and black (carbon). Hydrogen atoms and guest molecules present in the pores are omitted for clarity.

recently reported a synthetic procedure using microwave irradiation for the synthesis of MIL-47 and six other new vanadium metal−organic frameworks (V-MOFs).[16] The microwave synthesis[16] of MIL-47 is faster and gives higher yield (~25% in 10 min) than the previously published hydrothermal method (~15% in 4 days).[14] In this work, we used the previously developed microwave method[16] to grow MIL-47 crystals directly on electrospun fiber mats or powder-coated PAN films. We studied the growth of MIL-47 on polyacrylonitrile substrates as a function of microwave irradiation time using scanning electron microscopy (SEM), X-ray diffraction (XRD), Fourier transform infrared spectroscopy (FTIR), and X-ray photoelectron spectroscopy (XPS). The conversion of nitrile to carboxylic acid groups on the PAN surface was found to be a prerequisite for the growth of MIL-47 on the substrate. We reason that our method could usher in novel hydrid MOF-polymer materials, which could extend application of MOFs in fields such as filtration, chemical protective coatings, and catalysis.

2. Results and Discussion

A parallel-plate electrospinning apparatus[26] was used to electrospin a 10% PAN solution in *N*,*N*-dimethylformamide. The electrospun fibers were collected on a grounded aluminum foil, peeled off, folded, and finally hot-pressed (4.4×10^5 Pa) for 5 min at 200 °C to enhance the substrate's mechanical properties before the MOF functionalization. The PAN fiber morphology is preserved after the hot-pressing procedure (Figure S1 of the Supporting Information). Next, the PAN substrates were added at room temperature to vials containing terephthalic acid (TA), vanadium trichloride, and deionized water in 4:1:100 molar ratios and heated with microwaves (200 W) to 200 °C. The vials were irradiated for varying intervals of time from 5 s to 30 min. MOF crystals grew simultaneously on the PAN substrates and in the bulk solutions. The PAN substrates coated with MOF (hereafter termed MIL-47-sub) were removed from the solution, rinsed and soaked in deionized water (12 h), rinsed and soaked in methanol (24 h), and finally dried in an oven at 50 °C for 60 min before characterization. The crystals obtained in solution (hereafter, termed MIL-47-sol) were filtered and dried overnight in air before characterization.

The crystal morphology of MIL-47 grown on the electrospun fibers shows an interesting evolution as a function of synthesis time as observed with SEM (Figure 2a−e and Figure S2). After only 5 s, the polymer surface was partially covered with small agglomerates of MOF particles. Between 30 s and 3 min of reaction, the agglomerates grew as elongated anisotropic structures; after 6 min, the typical morphology of MIL-47 crystals was observed with little change up to 10 min. The fibers appear to have lost their identity and coalesced within the first 5 s of irradiation forming a more regular substrate. There was no noticeable difference between MOF crystals grown on electrospun PAN fibers and on cast films; in both cases, MOF crystals were found only on the substrate surface and not in the substrate bulk (Figure S3).

A PAN powder-coated substrate was prepared and patterned to highlight the role of the substrate polymer chemistry on the MOF growth. A fluoropolymer and a cross-linker were cast on a poly(ethylene terephthalate) (PET) substrate, and the fluoropolymer film was coated evenly with PAN powder prior to curing (for details, see the experimental section in the Supporting Information). This fluoropolymer offers excellent wettability and, when cross-linked with a multifunctional polyisocyanate, results in a rigid transparent film that possesses strong adhesion to both the PET substrate and the PAN powder. The film was cured at 70 °C overnight, resulting in a PAN-coated, laminated film, which was grooved on the PAN-coated side with a CNC machine to remove the PAN in some areas. The grooved PAN-coated film was added to a vial and irradiated with microwaves for 10 min. The microwave reaction described above resulted in the selective functionalization of the PAN-coated areas of the grooved, PAN powder-coated film with MIL-47 (Figure 2f).

Under the reaction conditions described above (water, 200 °C, pH = 1), PAN undergoes acid hydrolysis on the surface to give poly(acrylic acid),[27,28] and cross-linking in the bulk.[27] The carboxylic acid-functionalized PAN substrate shares the carboxylic functionality of the organic building block in MIL-47 and allows the material to grow. MIL-47 does not grow on Teflon, nor on PET, substrates that cannot be functionalized with carboxylic groups under the same conditions. As a control, a vial containing a PAN substrate, TA, deionized water (3 mL), and 5 drops of acid chloride (in place of VCl_3) was heated with microwaves (200 W) to 200 °C for 10 min. FTIR spectra indicate that the PAN substrate was functionalized successfully with TA molecules under these conditions, thus providing an

(26) Fridrikh, S. V.; Yu, J. H.; Brenner, M. P.; Rutledge, G. C. *Phys. Rev. Lett.* **2003**, *90*, 144502.

(27) Sebesta, F.; John, J.; Motl, A.; Stamberg, K. *Evaluation of Polyacrylonitrile (PAN) as a Binding Polymer for Adsorbers Used to Treat Liquid Radioactive Wastes*; Sandia National Laboratories: Albuquerque, NM, 1995; pp 5−11.

(28) Zil'berman, Y. N.; Starkov, A. A.; Pomerantseva, E. G. *Polym. Sci. U.S.S.R.* **1977**, *19*, 3135.

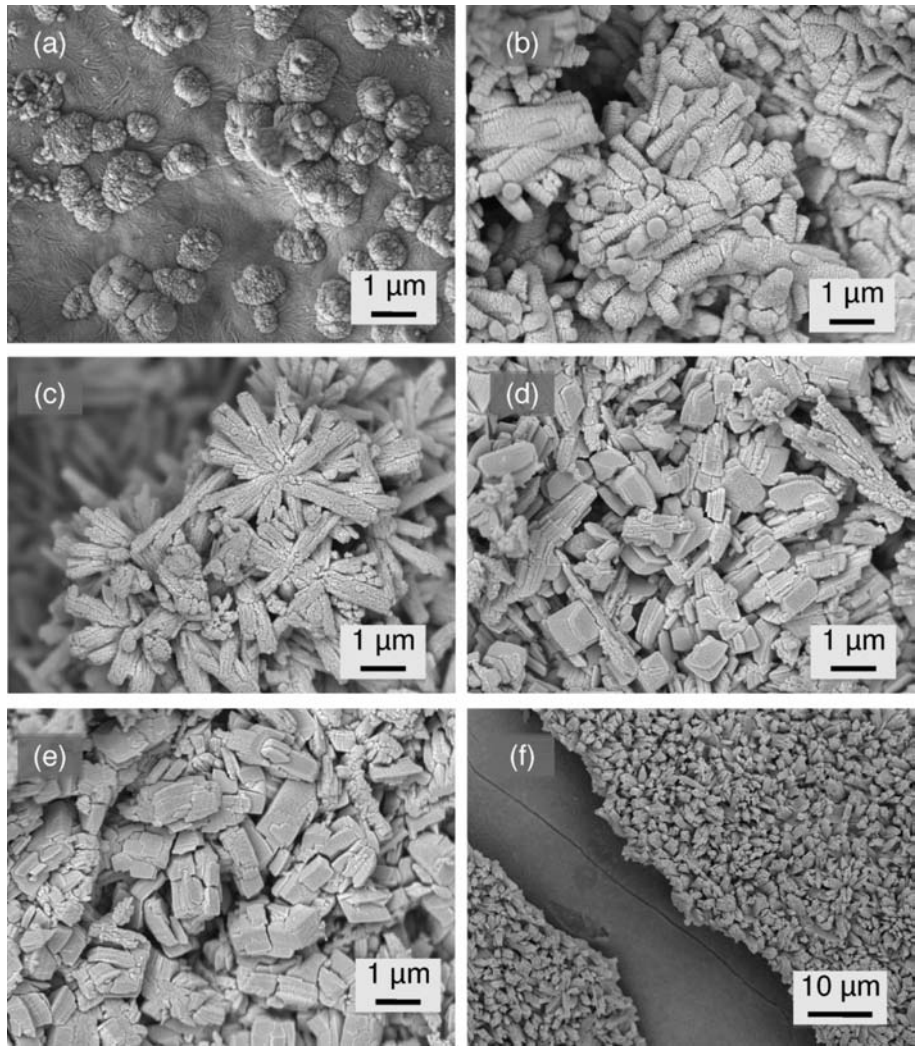

Figure 2. SEM images of polyacrylonitrile substrate prepared initially as an electrospun nanofiber mat, coated with MIL-47 material as a function of time: (a) 5 s, (b) 30 s, (c) 3 min, (d) 6 min, and (e) 10 min. Note that the initial fibers fused together and lost their identity very shortly after irradiation. (f) MIL-47-coated grooved PAN.

additional route for the carboxylic functionalization (Figure S4). For MIL-47-sub samples, the substrate color was whitish for reactions up to 10 min, while for longer syntheses and for the control experiment the color was red to brown, indicating for these latter cases the formation of conjugated compounds, possibly azopolyenes,[27,28] in the substrate bulk.

The difference in binding energy (Δ) between the O1s and $V2p_{3/2}$ levels in XPS spectra is widely used for determining the oxidation states of vanadium atoms in vanadium oxides[29] and was used to confirm that V^{3+} is the oxidation state of vanadium atoms in MIL-47.[16] The characteristic Δ values for V^{5+}, V^{4+}, V^{3+}, $V^{2+/1+}$, and V^{0} are 12.8, 14.16, 14.71, 16.33, and 17.65 eV $\pm$ 0.2 eV, respectively. The Δ values of MIL-47-sub samples indicate that after 5 s V^{3+} ions were already the primary constituent of the MOF material and remained so for all longer reaction times (Figure 3a).

The attenuated total reflection (ATR) FTIR spectra of MIL-47-sub samples (Figure 3b) show very little variation as a function of synthesis time and suggest that even after 5 s the material on the substrate was characterized by the same chemical groups and the same chemical connectivity as MIL-47. ATR exploits the evanescent field to probe the sample surface with a typical penetration depth between 0.5 and 3 μm if the sample is in good contact with the ATR crystal. Consistent with the SEM images, the PAN substrate peak is visible only for the first sample, obtained after 5 s, which was only partially covered with the MIL-47. The FTIR spectra also show that some TA molecules may have been included in the growing MOF film.

The amorphous PAN background and the preferred crystal orientation make the XRD characterization of MIL-47-sub samples difficult. Nevertheless, for the sample irradiated for 10 min (MIL-47-sub-10 m), the peak at 8.84°, characteristic of MIL-47, is clearly visible in the XRD pattern, while the pattern of the crystals simultaneously obtained in solution (MIL-47-sol-10 m) matches well the previously reported pattern for MIL-47[14,16] (Figure S5).

Because of the weak patterns obtained from the MIL-47-sub samples, we analyzed in detail the XRD pattern of MIL-47-sol samples as a function of the reaction time. The XRD patterns indicate that the samples were composed of a mixture of three phases: unreacted recrystallized TA,[14,16] a phase with broad peaks in the proximity of MIL-47 peaks, which we assigned to a disordered MIL-47 precursor phase, and MIL-47 (only for

(29) Silversmit, G.; Depla, D.; Poelman, H.; Marin, G. B.; De Gryse, R. *J. Electron Spectrosc. Relat. Phenom.* **2004**, *135*, 167–175.

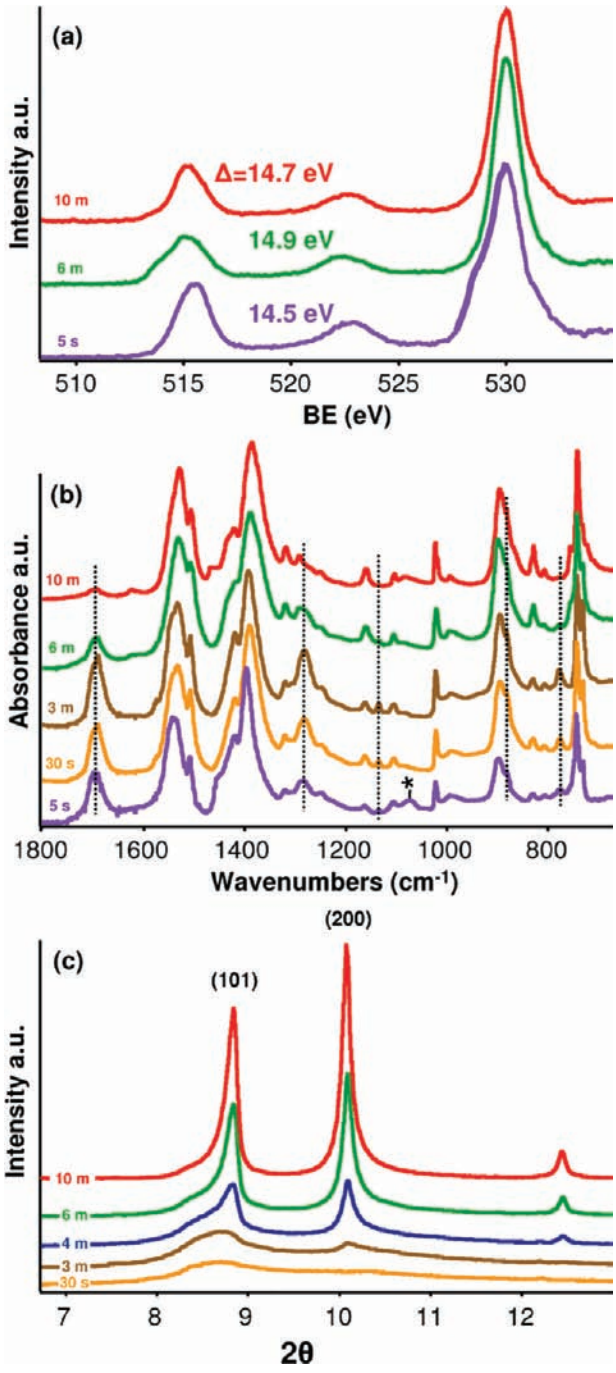

Figure 3. (a) XPS spectra and (b) FTIR spectra of MIL-47-coated PAN substrates prepared from electrospun nanofibers as a function of reaction time. (c) XRD diffraction patterns of MIL-47-sol materials as a function of the reaction time. 5 s (purple), 30 s (orange), 3 min (brown), 4 min (blue), 6 min (green), and 10 min (red). $\Delta = 14.71 \pm 0.2$ eV are typical values for V^{3+} atoms in vanadium oxide materials. In the FTIR spectra, the asterisk marks a peak belonging to the polyacrylonitrile substrate, while peaks belonging to terephthalic molecules are highlighted by dotted vertical lines. Data are displayed with an offset for clarity.

syntheses longer than 3 min). The fitting of the XRD pattern with these three phases was good (Figure S6); however, a systematic error was observed, due to the strong asymmetry of the (101), (202), (303) and possibly (301), (112), (302), (321), and (503) MIL-47 peaks (see Figure S7). It is likely that the peak asymmetries were caused by systematic crystal defects along specific directions, as observed in pillared clays due to planar disorder,[30] or multiwall carbon nanotubes, where the lack

Table 1. MIL-47 Unit Cell Parameters, Crystallite Size (*L*), and Intensity Ratio (*f*) as a Function of the Reaction Time[a]

time [min]	*a* [Å]	*b* [Å]	*c* [Å]	*L* [nm]	*f*
3	NA	NA	NA	90	0.07
4	17.511(5)	6.886(2)	12.170(2)	89	0.23
6	17.520(2)	6.890(1)	12.161(2)	85	0.43
10	17.535(3)	6.889(1)	12.152(1)	89	0.60

[a] *f* is defined as the ratio of the intensities (area) of all MIL-47 peaks to the total sum of the intensities of all precursor and MIL-47 peaks within the range of 2θ from 5° to 30°.

of correlation between carbon atoms in different layers produces an asymmetrical "sawtooth" shape to some peaks.[31] In MIL-47, VO chains are aligned in the [010] direction and lie in the (*h*0*l*) planes, while the terephthalic dicarboxylate ligands are aligned along the [*h*0*l*] direction (Figure 1). The asymmetrical shape to the (*h*0*l*) peaks indicates that, while the atoms were well ordered within any given (*h*0*l*) plane, the TA ligands were not fully ordered, suggesting the presence of connectivity defects between the chains. Other planes that exhibit some asymmetry are planes nearly parallel to the (*h*0*l*) planes.

We used mica as a reference standard to estimate the average crystallite size from the Williamson−Hull plot (Figures S8, S9). The Williamson−Hull analysis and the unit cell refinement (see Supporting Information for details) show that the MIL-47 average crystallite sizes and unit cell parameters do not change significantly as a function of the irradiation time (Table 1). From the Williamson−Hull plot, it appears in general that peaks corresponding to directions most closely parallel to [101] were broader than other peaks (Figure S9). This agrees with the hypothesis that the MIL-47 crystals are more disordered in the [101] direction, leading to smaller domain sizes.

The relative intensities of the peaks assigned to the precursor phase initially increase with respect to TA with increasing irradiation time, but decrease relative to the MIL-47 when the latter become observable (Table 1). The first, most intense MIL-47 peaks observable after 3 min of irradiation are assigned to the (200), (210), (020), and (420) planes. The crystalline order is thus obtained first in the (*hk*0) planes, which include the vanadium oxide chains. At the same time, the (*h*0*l*) planes (perpendicular to the chains) have systematically larger full widths at half maximum (fwhm's) and asymmetric peak shapes, indicating the presence of connectivity defects between the chains.

If the precursor phase were nanocrystalline MIL-47, we would expect to see a sharpening of peaks with irradiation time, reflecting a progressive crystal growth. Instead, the line profile analysis indicates that crystalline MIL-47 always has an average crystallite size of ~80 nm, with some subset of peaks corresponding to shorter domain lengths in the [101] direction. These observations, combined with FTIR and XPS data, show that MIL-47 grows at the expense of a disordered precursor phase that is made of the same building blocks but lacks long-range order. The long-range order is established initially along the vanadium oxide chains and eventually propagates on the perpendicular planes. This interpretation reflects the difficulty with which TA molecules are able to bind adjacent chains and results in a relatively large number of connectivity defects in the (*h*0*l*) planes.

(30) Gualtieri, A. F.; Ferrari, S.; Leoni, M.; Grathoff, G.; Hugo, R.; Shatnawi, M.; Paglia, G.; Billinge, S. *J. Appl. Crystallogr.* **2008**, *41*, 402–415.
(31) Zhou, O.; Fleming, R. M.; Murphy, D. W.; Chen, C. H.; Haddon, R. C.; Ramirez, A. P.; Glarum, S. H. *Science* **1994**, *263*, 1744–1747.

3. Conclusions

We report for the first time the synthesis and growth of a MOF material on a polymer substrate using fast microwave irradiation. The concomitant in situ functionalization of the PAN substrate with carboxylic acid groups is necessary for the MOF growth on the substrate. The combined SEM, FTIR, XPS, and XRD analysis provides evidence for the first time of MOF growth at the expense of an amorphous precursor phase, which is present even after only 5 s of microwave irradiation. This precursor phase is characterized by the same chemical groups, same chemical connectivity, and the same vanadium oxidation state as MIL-47 material. However, the precursor phase is not a nanocrystalline MIL-47 phase, but a closely related disordered phase. The present work demonstrates a novel technology to coat polymer fibers, sheets, films, etc., with functional materials such as MOFs. This technology could usher in novel applications of MOFs in fields such as filtration, chemical protective coatings, and catalysis.

Acknowledgment. This work was supported by the Novartis Center for Continuous Manufacturing. We thank Prof. Timothy Swager of MIT for the use of the microwave synthesizer. This work made use of the Shared Experimental Facilities supported by the MRSEC Program of the National Science Foundation under award number DMR-08-19762.

Supporting Information Available: Experimental section, additional SEM images, FTIR spectra, XRD pattern, and XRD analysis details. This material is available free of charge via the Internet at http://pubs.acs.org.

JA106381X